Bounded Error Schemes for the Wave Equation on Complex Domains

Saul Abarbanel,[1] **Adi Ditkowski,**[1] **and Amir Yefet**[1]

This paper considers the application of the method of boundary penalty terms (SAT) to the numerical solution of the wave equation on complex shapes with Dirichlet boundary conditions. A theory is developed, in a semi-discrete setting, that allows the use of a Cartesian grid on complex geometries, yet maintains the order of accuracy with only a linear temporal error-bound. A numerical example, involving the solution of Maxwell's equations inside a 2-D circular wave-guide demonstrates the efficacy of this method in comparison to others (e.g., the staggered Yee scheme)—we achieve a decrease of *two orders of magnitude* in the level of the L_2-error.

KEY WORDS: Finite difference; embedded methods; wave equation; FDTD.

1. INTRODUCTION

Hyperbolic systems of PDEs describing physical situations such as electromagnetism, acoustics, elastic waves, etc, may under many circumstances be cast as wave equations for the various field components.

One class of problems is that of solving numerically the Dirichlet problem on complex shapes, e.g., inside wave guides. For sufficiently non-simple geometries, the option of transforming the problem to body-fitted coordinates is not always a viable option, especially in three space dimensions. There are other options, such as using Cartesian grids and approximating the body shape via "staircasing", "diagonal split cell model", etc. (see for example Chapter 10 in [4]). It is well known that these devices are not very efficacious, particularly in the high frequency regime. We shall demonstrate that "staircasing" can fail even for low frequencies.

─────────
[1] Department of Applied Mathematics, School of Mathematical Sciences, Tel-Aviv University, Tel-Aviv, Israel. E-mail: adid@post.tau.ac.il

In this paper, we consider the application of the method of boundary penalty terms (SAT, see [1–3]) to the numerical solution of the wave equation in a finite domain with Dirichlet boundary conditions.

In Sec. 2, we develop the theory that allows us to use a Cartesian grid on complex geometries and yet maintain the order accuracy with a linear temporal error-bound.

In Sec. 3, we construct a second-order accurate scheme that fulfills the conditions imposed by the theory presented in Sec. 2.

Section 4 is devoted to a numerical example—the solution of the transverse magnetic (TM) Maxwell's equations [4] between two concentric circles (This configuration might be considered as a cross-section of a very long wave-guide.) This problem is solved using four different numerical algorithms. Two of them solve the first order system with "staircasing"—the Yee staggered scheme [7] and a fourth-order spatially staggered scheme due to Turkel and Yefet [5,6]. The other two solve the wave equation directly on a non-staggered Cartesian grid, one with the SAT formulation and one without. All three "standard" (non-SAT) algorithms have very large errors; the SAT algorithm has errors that are at least two order of magnitude smaller. Summary and conclusions, and ideas for future work are presented in Sec. 5.

2. THEORETICAL FRAMEWORK OF THE METHOD

In [1–3], it was shown how the case of a one-dimensional PDE can be used as a building block for the multidimensional case for constructing error-bounded algorithms over complex geometries with Dirichlet boundary condition. We therefore start with the following one-dimensional problem:

$$\frac{\partial^2 u}{\partial t^2} = \frac{\partial^2 u}{\partial x^2} + f(x,t), \quad \Gamma_L \leqslant x \leqslant \Gamma_R, \quad t > 0, \tag{2.1}$$

$$u(x,0) = u_0(x), \tag{2.1a}$$

$$\frac{\partial}{\partial t} u(x,0) = u_{t_0}(x), \tag{2.1b}$$

$$u(\Gamma_L, t) = g_L(t), \tag{2.1c}$$

$$u(\Gamma_R, t) = g_R(t) \tag{2.1d}$$

and $f(x,t) \in C^2$.

Let us discretize (2.1) spatially on the uniform grid presented in Fig. 1. Note that the boundary points do not necessarily coincide with
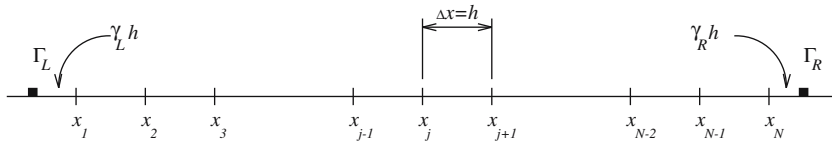
Fig. 1. One-dimensional grid.

x_1 and x_N. Set $x_{j+1} - x_j = h$, $1 \leqslant j \leqslant N - 1$; $x_1 - \Gamma_L = \gamma_L h$, $0 \leqslant \gamma_L < 1$; $\Gamma_R - x_N = \gamma_R h$, $0 \leqslant \gamma_R < 1$.

Since, unlike the cases discussed in [1, 2], Eq. (2.1) has a second time derivative, attempts to apply naively the methods presented there fail. The reason is that if we follow the procedure used there and write the following discrete approximation to (2.1),

$$\frac{d^2}{dt^2}\mathbf{u} = D\mathbf{u} + \mathbf{f}(t) + \mathbf{T}_e, \tag{2.2}$$

where $\mathbf{u}$ is the projection of the exact solution $u(x, t)$ onto the grid, i.e. $u(x_j, t) = u_j(t) \overset{\triangle}{=} \mathbf{u}(t)$; and write the numerical scheme

$$\frac{d^2\mathbf{v}}{dt^2} = \left[D\mathbf{v} - \tau_L(A_L\mathbf{v} - \mathbf{g}_L) - \tau_R(A_R\mathbf{v} - \mathbf{g}_R) \right] + \mathbf{f}(t), \tag{2.3}$$

then the equation for the error vector $\boldsymbol{\epsilon} = \mathbf{u} - \mathbf{v}$ becomes

$$\frac{d^2\,\boldsymbol{\epsilon}}{dt^2} = M\,\boldsymbol{\epsilon} + \mathbf{T}. \tag{2.4}$$

In the above, $\mathbf{v}$ is the numerical approximation to $\mathbf{u}$, and

$$M = D - \tau_L A_L - \tau_R A_R. \tag{2.5}$$

D is a differentiation matrix of the proper order of accuracy that does not use boundary values. The matrices A_L and A_R are defined by the relations

$$A_L\mathbf{u} = \mathbf{g}_L - \mathbf{T}_L, \qquad A_R\mathbf{u} = \mathbf{g}_R - \mathbf{T}_R, \tag{2.6}$$

i.e., each row in $A_L(A_R)$ is composed of the coefficients extrapolating $\mathbf{u}$ to its boundary value $g_L(g_R)$ at $\Gamma_L(\Gamma_R)$ to within the order of accuracy (The error is then $T_L(T_R)$.) The diagonal matrices τ_L and τ_R are given by

$$\tau_L = \mathrm{diag}(\tau_{L_1}, \tau_{L_2}, \dots, \tau_{L_N}), \qquad \tau_R = \mathrm{diag}(\tau_{R_1}, \tau_{R_2}, \dots, \tau_{R_N}).$$

The constrain on the construction of the As, τs and D is that M in (2.4) be negative definite. The negative definiteness of M is a necessary condition for extending the 1-D theory to the multidimensional case (see [1, 3]). Also in (2.4)

$$\mathbf{T} = \mathbf{T}_e - \tau_L \mathbf{T}_L - \tau_R \mathbf{T}_R = (T_1, T_2, \ldots, T_m, \ldots, T_N)^T. \tag{2.7}$$

If the matrix M can be diagonalized*, then

$$M = Q^{-1} \Lambda Q \tag{2.8}$$

with the diagonal matrix, Λ, having the eigenvalues of M. Defining $\boldsymbol{\mu} = Q\,\boldsymbol{\epsilon}$, Eq. (2.4) becomes

$$\begin{aligned}
\frac{d^2\,\boldsymbol{\mu}}{dt^2} &= \Lambda\,\boldsymbol{\mu} + Q\mathbf{T} \\
&= \Lambda\,\boldsymbol{\mu} + \hat{\mathbf{T}}.
\end{aligned} \tag{2.9}$$

This is an un-coupled system of ODEs. The general solution for the mth equation is:

$$\mu_m(t) = c_{m_1} e^{\sqrt{\lambda_m}\,t} + c_{m_2} e^{-\sqrt{\lambda_m}\,t} + \frac{1}{\sqrt{\lambda_m}} \int_0^t \sinh\left(\sqrt{\lambda_m}(t-s)\right) \hat{T}_m(s)\,ds.$$

Recalling that at $t=0$, $\boldsymbol{\epsilon} = \boldsymbol{\epsilon}_t = 0$ (i.e. $\boldsymbol{\mu} = \boldsymbol{\mu}_t = 0$ at $t=0$), the solution of (2.9) becomes:

$$\mu_m(t) = \frac{1}{\sqrt{\lambda_m}} \int_0^t \hat{T}_m(s) \sinh\left[\sqrt{\lambda_m}(t-s)\right] ds. \tag{2.10}$$

Note that unless all the eigenvalues of M are real and non-positive some of the $\sqrt{\lambda_m}$'s will have a positive real part, in which that case at least one of the μ_m's may grow exponentially in time. In order to prevent this, we have to demand that M, in addition to being negative definite, also possess only real eigenvalues. Furthermore, in order to use the 1-D scheme as a building block for multidimensional schemes, M should be built in a way that verifies that the property of real negative eigenvalues carries over to the multi-dimensional differentiating matrix. One way to achieve this goal is to construct M as a negative-definite *symmetric* matrix. Then

---

*Extensive numerical evidence has shown that the M in [1, 2] (i.e. representing the second derivative to Fourth- and Second-order accuracy, respectively) has distinct eigenvalues and hence is diagonalizable.

an estimate on the error bound can be derived directly from the solution (2.10),

$$|\mu_m(t)| \leqslant \frac{1}{\sqrt{|\lambda_m|}} \hat{T}_{m_M} t,$$

where $\hat{T}_{m_M} = \max_{0 \leqslant s \leqslant t} |\hat{T}_m(s)|$. Then, for a normalized Q,

$$\| \boldsymbol{\epsilon} \| = \| \boldsymbol{\mu} \| \leqslant \frac{1}{c_0} \| \hat{\mathbf{T}}_M \| t, \tag{2.11}$$

where $c_0 = \min_{m=1,\ldots,N} \sqrt{|\lambda_m|}$. Therefore $\| \boldsymbol{\epsilon} \|$ grows at most linearly with t.

This result, of a linear temporal bound on the error-norm, can also be derived by resorting to energy method (see [3]), instead of directly from the solution.

Also, as mentioned before, the construction of multi-dimensional case

$$\frac{\partial^2 u}{\partial t^2} = \nabla^2 u + f(\mathbf{x}, t),$$

on complex shapes is completely analogous to the method indicated in [1, 3].

3. CONSTRUCTION OF THE SCHEME

This section is devoted to the task of constructing a symmetric negative definite matrix M for the case of a second order accurate finite difference algorithm.

Let

$$D = \frac{1}{h^2} \left\{ \begin{bmatrix} 1 & -2 & 1 & 0 & & & & & \\ 1 & -2 & 1 & 0 & & & & & \\ 0 & 1 & -2 & 1 & & & & & \\ 0 & 0 & 1 & -2 & 1 & & & & \\ & & & & \ddots & \ddots & \ddots & & \\ & & & & & 1 & -2 & 1 & 0 & 0 \\ & & & & & & 1 & -2 & 1 & 0 \\ & & & & & & & 1 & -2 & 1 \\ & & & & & & & 1 & -2 & 1 \end{bmatrix} \right.$$

$$+ \begin{bmatrix} 0 & & & & & \\ & c_2 & & & & \\ & & c_3 & & & \\ & & & \ddots & & \\ & & & & c_{N-2} & \\ & & & & & c_{N-1} & \\ & & & & & & 0 \end{bmatrix} \begin{bmatrix} 0 & 0 & 0 & 0 & & & \\ 1 & -3 & 3 & -1 & & & \\ -1 & 4 & -6 & 4 & -1 & & \\ & \ddots & \ddots & \ddots & \ddots & \ddots & \\ & & -1 & 4 & -6 & 4 & -1 \\ & & & -1 & 3 & -3 & 1 \\ & & & 0 & 0 & 0 & 0 \end{bmatrix}$$

$$-\tilde{c} \begin{bmatrix} 0 & 0 & 0 & & & & \\ 0 & 1 & -2 & 1 & & & \\ -1 & 2 & 0 & -2 & 1 & & \\ & \ddots & \ddots & \ddots & \ddots & \ddots & \\ & & -1 & 2 & 0 & -2 & 1 \\ & & & -1 & 2 & -1 & 0 \\ & & & 0 & 0 & 0 & 0 \end{bmatrix} \Bigg\}, \tag{3.1}$$

where

$$c_k = c_2 + \frac{c_{N-1} - c_2}{N-3}(k-2) \tag{3.2}$$

and

$$\tilde{c} = \frac{c_{N-1} - c_2}{N-3}. \tag{3.3}$$

Note, that as in [2] and [3], we had to resort to using *connectivity terms*, the last two matrices in (3.1).

$$A_L = \begin{bmatrix} \frac{1}{2}(2+\gamma_L)(1+\gamma_L) & -\gamma_L(2+\gamma_L) & \frac{1}{2}(\gamma_L+\gamma_L^2) & 0 & \dots & 0 \\ \vdots & \vdots & \vdots & \vdots & & \vdots \\ \frac{1}{2}(2+\gamma_L)(1+\gamma_L) & -\gamma_L(2+\gamma_L) & \frac{1}{2}(\gamma_L+\gamma_L^2) & 0 & \dots & 0 \end{bmatrix}, \tag{3.4}$$

$$A_R = \begin{bmatrix} 0 & \dots & 0 & \frac{1}{2}(\gamma_R+\gamma_R^2) & -\gamma_R(2+\gamma_R) & \frac{1}{2}(2+\gamma_R)(1+\gamma_R) \\ \vdots & \vdots & \vdots & \vdots & & \vdots \\ 0 & \dots & 0 & \frac{1}{2}(\gamma_R+\gamma_R^2) & -\gamma_R(2+\gamma_R) & \frac{1}{2}(2+\gamma_R)(1+\gamma_R) \end{bmatrix}. \tag{3.5}$$

$$\tau_L = \frac{1}{h^2} \text{diag} \left[\tau_{L_1}, \tau_{L_2}, \tau_{L_3}, 0, \dots, 0, 0 \right], \tag{3.6}$$

$$\tau_R = \frac{1}{h^2} \text{diag} \left[0, 0, \dots, 0, \tau_{R_{N-2}}, \tau_{R_{N-1}}, \tau_{R_N} \right]. \tag{3.7}$$

In order to make the matrix $M = D - \tau_L A_L - \tau_R A_R$ symmetric we choose:

$$c_2 = \frac{(1-\gamma_L)\,\gamma_L}{2},$$

$$c_{N-1} = \frac{(1-\gamma_R)\,\gamma_R}{2},$$

$$\tau_{L_2} = \frac{3 - \gamma_L - 2\,\gamma_L\,\tau_{L_1}}{1+\gamma_L},$$

$$\tau_{L_3} = \frac{-2 + \gamma_L + \gamma_L\,\tau_{L_1}}{2+\gamma_L}, \tag{3.8}$$

$$\tau_{R_{N-1}} = \frac{3 - \gamma_R - 2\,\gamma_R\,\tau_{R_N}}{1+\gamma_R},$$

$$\tau_{R_{N-2}} = \frac{-2 + \gamma_R + \gamma_R\,\tau_{R_N}}{2+\gamma_R}$$

and in order to make the matrix M negative definite we take

$$\tau_{L_1},\ \tau_{R_N} \geqslant 4. \tag{3.9}$$

The proof that the symmetric matrix M is indeed negative-definite is given in the Appendix to this paper.

Note also that instead of solving (2.3) directly as a second-order ODE system in time, one can solve

$$\frac{d\mathbf{w}}{dt} = [D\mathbf{v} - \tau_L(A_L\mathbf{v} - \mathbf{g}_L) - \tau_R(A_R\mathbf{v} - \mathbf{g}_R)] + \mathbf{f},$$

$$\frac{d\mathbf{v}}{dt} = \mathbf{w}. \tag{3.10}$$

The number of 'variables' has increased from N to $2N$ but one gains in the simplicity of the time integration.

4. NUMERICAL EXAMPLE

We consider the dimensionless Maxwell's equation for TM field (see [4, pp. 51–56]) in two space dimensions:

$$\frac{\partial E}{\partial t} = \frac{\partial H_y}{\partial x} - \frac{\partial H_x}{\partial y}, \tag{4.1}$$

$$\frac{\partial H_x}{\partial t} = -\frac{\partial E}{\partial y}, \tag{4.2}$$

$$\frac{\partial H_y}{\partial t} = \frac{\partial E}{\partial x}, \tag{4.3}$$

where H_x and H_y are the x and y components of the magnetic vector, $\mathbf{H}$, and E is the electric field in the z-direction. The set (4.1)–(4.3) is to be solved in the space between two concentric circles, $\frac{1}{6} < r < \frac{1}{2}$. We consider the case of perfectly conducting boundaries. Thus the boundary conditions are given by

$$E(\tfrac{1}{2}, \theta, t) = 0, \tag{4.4}$$

$$E(\tfrac{1}{6}, \theta, t) = 0. \tag{4.5}$$

We choose the following initial conditions (note the polar coordinates r, θ):

$$E(r, \theta, 0) = \cos\theta \, [J_1(\omega r) + a \, Y_1(\omega r)], \tag{4.6}$$

$$
\begin{aligned}
H_y(r, \theta, 0) = & -\sin 2\theta \Big\{ \frac{1}{2\omega r} [J_1(\omega r) + a \, Y_1(\omega r)] \\
& - \frac{1}{4} [J_0(\omega r) - J_2(\omega r) + a \, Y_0(\omega r) - a \, Y_2(\omega r)] \Big\},
\end{aligned} \tag{4.7}
$$

$$
\begin{aligned}
H_x(r, \theta, 0) = & \frac{\cos^2\theta}{\omega r} [J_1(\omega r) + a \, Y_1(\omega r)] \\
& - \frac{\sin^2\theta}{2} [J_0(\omega r) - J_2(\omega r) + a \, Y_0(\omega r) - a \, Y_2(\omega r)],
\end{aligned} \tag{4.8}
$$

where the J_n's and the Y_n's are Bessel functions of the first and second kind of order n, respectively. Also,

$$a \cong 1.76368380110927, \qquad \omega \cong 9.813695999428405. \tag{4.9}$$

The exact solution of the IBV problem (4.1)–(4.8) is given by:

$$E(r, \theta, t) = \cos(\omega t + \theta) [J_1(\omega r) + a \, Y_1(\omega r)], \tag{4.10}$$

$$
\begin{aligned}
H_y(r, \theta, t) = & -\frac{1}{\omega r} \cos\theta \cos(\omega t + \theta) [J_1(\omega r) + a \, Y_1(\omega r)] \\
& + \tfrac{1}{2} \cos\theta \sin(\omega t + \theta) [J_0(\omega r) - J_2(\omega r) + a \, Y_0(\omega r) - a \, Y_2(\omega r)],
\end{aligned} \tag{4.11}
$$

$$
\begin{aligned}
H_x(r, \theta, t) = & \frac{1}{\omega r} \cos\theta \cos(\omega t + \theta) [J_1(\omega r) + a \, Y_1(\omega r)] \\
& - \tfrac{1}{2} \sin\theta \sin(\omega t + \theta) [J_0(\omega r) - J_2(\omega r) + a \, Y_0(\omega r) - a \, Y_2(\omega r)].
\end{aligned} \tag{4.12}
$$

We note that we can extract from (4.1) to (4.3) a wave equation for the electric field E,

$$\frac{\partial^2 E}{\partial t^2} = \frac{\partial^2 E}{\partial x^2} + \frac{\partial^2 E}{\partial y^2}. \tag{4.13}$$

The boundary conditions on E in (4.13) are given by (4.4)–(4.5). The initial condition $E(r, \theta, 0)$ is given by (4.6). We need an additional initial condition on E_t, which we obtain by differentiating (4.10), namely

$$E_t(r, \theta, 0) = -\omega \sin \theta \left[J_1(\omega r) + a\, Y_1(\omega r) \right]. \tag{4.14}$$

Four numerical schemes were used to solve the problem:

(i) The Yee scheme [7]. This second order accurate scheme is staggered both in space and time. This entails putting initial conditions of H_x and H_y at $\Delta t/2$ rather than at $t=0$. These initial conditions are derived from the exact solution. The numerical solution is carried out on the "staircased" domain shown in Fig. 2.

(ii) A modification of the Yee scheme (designated $Ty(2, 4)$) (see [5,6]). This one has fourth-order spatial accuracy and second-order in time. The stagger is maintained as before, with the same "staircased" domain.

(iii) The SAT algorithm for the wave equation described in Secs. 2 and 3. The grid used for the numerical integration is shown in
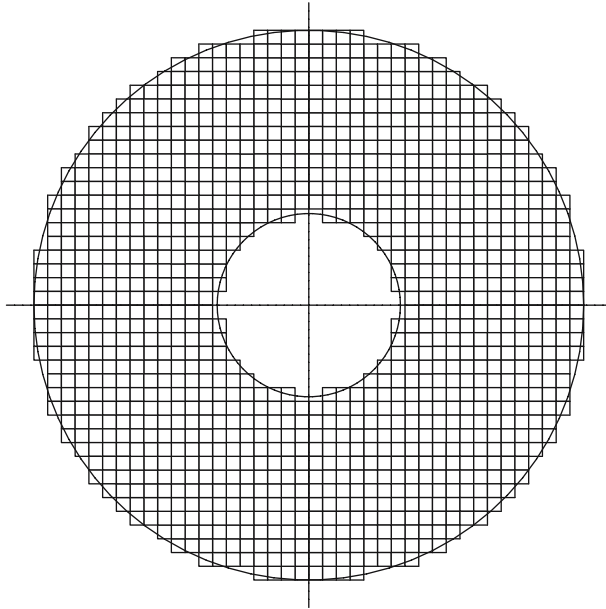
Fig. 2. The "staircased" domain, $h = 1/40$.
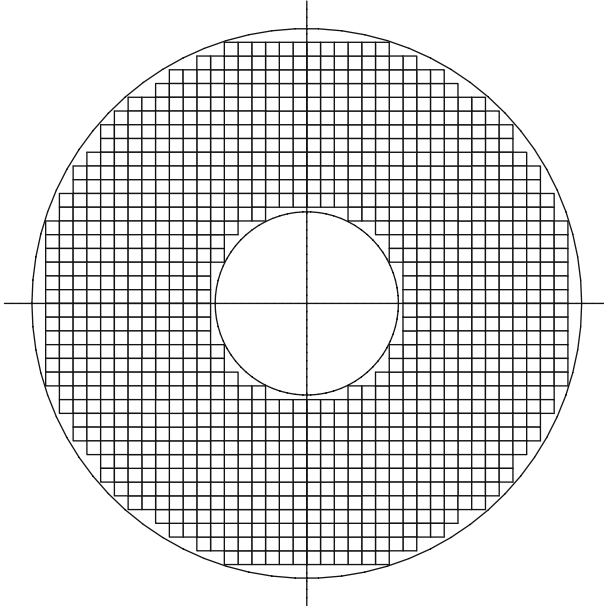
Fig. 3. The embedded grid, $h = 1/40$.

Fig. 3. The time evolution is done by a fourth-order Runge–Kutta method.

(iv) An algorithm which formally looks like the SAT in (iii), but is applied to the "staircased" domain of Fig. 2 (rather than Fig. 3). To order $O(h^2)$, this is equivalent to using a standard spatial central differencing scheme with the nodal points at edges of the domain given the boundary value zero. The time integration is done as in the case (iii).

We first present the L_2 error in E for all four schemes at $t = 1$ and 10 for the cases $\Delta x = \Delta y = h = 1/40$, $h = 1/80$ and $h = 1/160$ (see Table I).

It is immediately apparent from the table that the SAT-error (scheme (iii)) *is at least two orders of magnitude smaller* than that of the other three algorithms at all the various times and grid spacings.

Since the non-SAT schemes have errors which are unacceptably large we do not show details of their temporal behavior. The SAT algorithm (scheme (iii)) has an L_2 error which grows in time as shown in Fig. 4. We see that this temporal growth is bound by a linear curve, whose slope depends on h. We note that for all reasonable dimensionless time the error is quite small, especially for $h \leqslant 1/80$.

Table I.   The L_2 Error

		$h=1/40$	$h=1/80$	$h=1/160$	Convergence rate
$t=1$					
i	Yee	0.4322	0.3635	0.1742	0.66
ii	Ty(2,4)	0.4038	0.3347	0.1579	0.68
iii	SAT	0.001203	0.0001705	1.5019e-05	3.16
iv	Staircased	0.1022	0.05041	0.01936	1.20
$t=10$					
i	Yee	0.5101	0.4364	0.6683	Not applicable
ii	Ty(2,4)	0.2642	0.7079	0.7243	Not applicable
iii	SAT	0.008435	0.0008354	8.2707e-05	3.33
iv	Staircased	0.7929	0.4735	0.7829	Not applicable
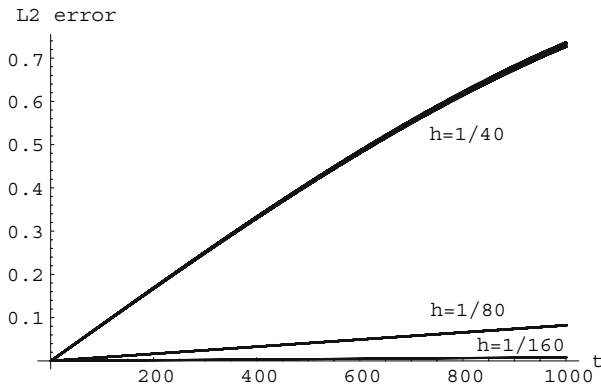
Fig. 4.   SAT, L_2 error versus time.

5. CONCLUSIONS AND DISCUSSION

(i)   It can be seen from Table I, that the "staircasing" approxima-
tion causes large errors. It reduces the accuracy to first order
or less. At $t=10$ the errors are so large that no convergence is
obtained. Even the SAT scheme when run on the "staircased"
domain, it presents poor convergence. On the other hand,
when the SAT scheme is run on the true domain, it converge
properly.

(ii)   The numerical results validate the theoretical predictions of the temporal behavior of the L_2 norm of the error.

(iii) Grosso-modo the CPU time per node is of the same order for all schemes.

(iv)   The results from Table I and Fig. 4 seem to indicate that the scheme (iii) converges as h^3, although the algorithm has a truncation error of order h^2. We do not understand this pleasant anomaly, although it is possible that even with $h = 1/160$ we are not yet in the asymptotic convergence regime.

(v)   In the future, we would like to apply the SAT methodology directly to hyperbolic systems such as (4.1)–(4.3). The theory is not complete yet.

ACKNOWLEDGMENTS

APPENDIX A

We decompose the matrix M, defined in (2.5) and (3.1)–(3.8) as follows:

$$M = \frac{1}{h^2} \left[\alpha M_1 + (1 - \alpha) M_2 + M_3 + M_4 + M_5 \right], \tag{5.1}$$

where

$$M_1 = \begin{bmatrix} -2 & 1 & & & & & \\ 1 & -2 & 1 & & & & \\ & 1 & -2 & 1 & & & \\ & & \ddots & \ddots & \ddots & & \\ & & & 1 & -2 & 1 & \\ & & & & 1 & -2 & 1 \\ & & & & & 1 & -2 \end{bmatrix}, \tag{5.2}$$

$$
M_2 =
\begin{bmatrix}
0 & 0 & 0 \\
0 & 0 & 0 \\
0 & 0 & -1 & 1 \\
& & 1 & -2 & 1 \\
& & & \ddots & \ddots & \ddots \\
& & & & 1 & -2 & 1 \\
& & & & 0 & 1 & -1 & 0 & 0 \\
& & & & & & & 0 & 0 & 0 \\
& & & & & & & 0 & 0 & 0
\end{bmatrix},
\tag{5.3}
$$

$$
M_3 = -\left\{
\begin{bmatrix}
0 & 0 & 0 \\
0 & -1 & 1 \\
0 & 1 & -2 & 1 \\
& & \ddots & \ddots & \ddots \\
& & & 1 & -2 & 1 & 0 \\
& & & & 1 & -1 & 0 \\
& & & & 0 & 0 & 0
\end{bmatrix}
\right.
$$

$$
\left.
\begin{bmatrix}
0 \\
& c_2 \\
& & c_3 \\
& & & \ddots \\
& & & & c_{N-2} \\
& & & & & c_{N-1} \\
& & & & & & 0
\end{bmatrix}
\begin{bmatrix}
0 & 0 & 0 \\
0 & -1 & 1 \\
0 & 1 & -2 & 1 \\
& & \ddots & \ddots & \ddots \\
& & & 1 & -2 & 1 & 0 \\
& & & & 1 & -1 & 0 \\
& & & & 0 & 0 & 0
\end{bmatrix}
\right\},
\tag{5.4}
$$

$$
M_4 =
\begin{bmatrix}
m_4^{1,1} & m_4^{1,2} & m_4^{1,3} \\
m_4^{1,2} & m_4^{2,2} & m_4^{2,3} & 0 \\
m_4^{1,3} & m_4^{2,3} & m_4^{3,3} \\
\\
& 0 & & 0
\end{bmatrix},
\tag{5.5}
$$

where

$$
\begin{aligned}
m_4^{1,1} &= 1 + 2\alpha - \frac{(1+\gamma_L)(2+\gamma_L)\tau_{L_1}}{2}, \\
m_4^{1,2} &= -2 - \alpha + \gamma_L(2+\gamma_L)\tau_{L_1}, \\
m_4^{1,3} &= 1 - \frac{\gamma_L(1+\gamma_L)\tau_{L_1}}{2},
\end{aligned}
$$

$$m_4^{2,2} = 2\alpha + \frac{7\gamma_L - 4\left(1+\gamma_L^2\right) - \gamma_L^2\left(2+\gamma_L\right)\left(1+4\tau_{L_1}\right)}{2\left(1+\gamma_L\right)},$$

$$m_4^{2,3} = 1 - \alpha - \frac{3\gamma_L}{2} + \frac{\gamma_L^2}{2} + \gamma_L^2\tau_{L_1},$$

$$m_4^{3,3} = 2\alpha + \frac{-4 + \gamma_L^2 - \gamma_L^3 - \gamma_L^2\left(1+\gamma_L\right)\tau_{L_1}}{2\left(2+\gamma_L\right)}$$

and

$$M_5 = \begin{bmatrix} 0 & & 0 & \\ & m_5^{N-2,N-2} & m_5^{N-1,N-2} & m_5^{N,N-2} \\ 0 & m_5^{N-1,N-2} & m_5^{N-1,N-1} & m_5^{N,N-1} \\ & m_5^{N,N-2} & m_5^{N,N-1} & m_5^{N,N} \end{bmatrix}, \tag{5.6}$$

where

$$m_5^{N,N} = 1 + 2\alpha - \frac{\left(1+\gamma_R\right)\left(2+\gamma_R\right)\tau_{R_N}}{2},$$

$$m_5^{N,N-1} = -2 - \alpha + \gamma_R\left(2+\gamma_R\right)\tau_{R_N},$$

$$m_5^{N,N-2} = 1 - \frac{\gamma_R\left(1+\gamma_R\right)\tau_{R_N}}{2},$$

$$m_5^{N-1,N-1} = 2\alpha + \frac{7\gamma_R - 4\left(1+\gamma_R^2\right) - \gamma_R^2\left(2+\gamma_R\right)\left(1+4\tau_{R_N}\right)}{2\left(1+\gamma_R\right)},$$

$$m_5^{N-1,N-2} = 1 - \alpha - \frac{3\gamma_R}{2} + \frac{\gamma_R^2}{2} + \gamma_R^2\tau_{R_N},$$

$$m_5^{N-2,N-2} = 2\alpha + \frac{-4 + \gamma_R^2 - \gamma_R^3 - \gamma_R^2\left(1+\gamma_R\right)\tau_{R_N}}{2\left(2+\gamma_R\right)}.$$

The matrix M_1 is negative-definite and bounded away from 0 by $h^2\pi^2$ by the argument leading to Eq. (2.4.31), see appendix to chapter 2 in [3]. M_2 is non-positive definite, see Eqs. (2.4.34) and (2.4.35) in that appendix. From (3.2), (3.3) and (3.8) follows that $c_k \geqslant 0$, $k = 1, \ldots, N$, therefore, the matrix M_3 is non-positive. For a given value of $0 \leqslant \alpha \leqslant 1$, τ_{L_1} and τ_{R_N} can be found such that the matrices M_4 and M_5 will be non-positive, for all γ_L and γ_R. For example: for $\alpha = 1/10$, $\tau_{L_1} = \tau_{R_N} = 4$; for $\alpha = 1/2$, $\tau_{L_1} = \tau_{R_N} = 9$ and for $\alpha = 8/10$, $\tau_{L_1} = \tau_{R_N} = 24$. This completes the proof that M is indeed a negative-definite matrix, bounded away from 0 by $\alpha\pi^2$. Therefore the

norm of the error vector $\| \epsilon \|$ can grow at most linearly in time, see Eq. (2.11).

REFERENCES

1. Abarbanel, S., and Ditkowski, A., (1997). Asymptotically stable fourth-order accurate schemes for the diffusion equation on complex shapes. *J. Comput. Phys.* **133**(2). Also, Multi-Dimensional Asymptotically Stable Fourth-Order Accurate Schemes for the Diffusion Equation. ICASE Report No. 96-8, February 1996.
2. Abarbanel, S., and Ditkowski, A., Multi-dimensional asymptotically stable schemes for advection–diffusion equations.ICASE Report 47-96. To appear *Comput. Fluids*.
3. Ditkowski, A., (1997). *Bounded-error finite difference schemes for initial boundary value problems on complex domains*, Thesis, Department of Applied Mathematics, School of Mathematical Sciences, Tel-Aviv University, Tel-Aviv, Israel.
4. Taflove, A., (1995). Computational Electrodynamics, The Finite-Difference Time-Domain Method. Artech House Inc., pp. 51–56.
5. Turkel, E., and Yefet, A., (2000). Fourth Order Compact Implicit Method for the Maxwell Equations with Discontinuous. *IEEE Trans. Antennas Propagat.* **33**, 125–134.
6. Turkel, E., and Yefet, A., (2000). On the construction of a high order difference scheme for the complex domain in cartesian grid. *Appl. Numer. Math.* **33**, 113–124.
7. Yee, K. S., (1966). Numerical solution of initial boundary value problems involving Maxwell's equations in isotropic media. *IEEE Trans. Antennas Propagat.* **AP-14**(4), 302–307.